Element-free Galerkin method for a kind of KdV equation*

Wang Ju-Feng(王聚丰)[a)†], Sun Feng-Xin(孙凤欣)[b)], and Cheng Rong-Jun(程荣军)[a)]

[a)] *Ningbo Institute of Technology, Zhejiang University, Ningbo* 315100, *China*
[b)] *Ningbo University of Technology, Ningbo* 315016, *China*

(Received 26 May 2009; revised manuscript received 28 December 2009)

The present paper deals with the numerical solution of the third-order nonlinear KdV equation using the element-free Galerkin (EFG) method which is based on the moving least-squares approximation. A variational method is used to obtain discrete equations, and the essential boundary conditions are enforced by the penalty method. Compared with numerical methods based on mesh, the EFG method for KdV equations needs only scattered nodes instead of meshing the domain of the problem. It does not require any element connectivity and does not suffer much degradation in accuracy when nodal arrangements are very irregular. The effectiveness of the EFG method for the KdV equation is investigated by two numerical examples in this paper.

Keywords: element-free Galerkin method, meshless method, KdV equation
PACC: 0200, 0260, 4410

1. Introduction

In 1895, Korteweg and de Vries[1] derived the famous equation, the KdV equation, for the propagation of waves in one dimension on the surface of water. The KdV equation is a balance between time evolution, nonlinearity and dispersion. This is one of the most useful nonlinear partial differential model equations for solitary waves, and can be used to describe many important physical phenomena, some examples of which are shallow water waves, ion acoustic plasma waves, bubble-liquid mixtures, and wave phenomena in harmonic crystals.[2]

Because of its broad application, the KdV equation has attracted much attention and research. Under an appropriate initial condition, Gardner *et al.*[3] have shown the existence and uniqueness of solutions of the KdV equation. Analytical solutions of the KdV equation have also been obtained for some special initial conditions.[4−8] But in many cases, it is very difficult to find the analytical solutions. So the only choice left is the approximate numerical solution. The numerical methods for the KdV equation are mainly based on mesh-methods, such as the finite difference method, the finite element method, the finite volume method, and so on.[9−11]

The mesh-methods are robust and thoroughly developed techniques, but they are not without shortcomings. The reliance of the method on a mesh leads to complications for certain classes of problems, such as large deformation processes. To ameliorate these difficulties, meshless methods have been developed. These methods do not require a mesh to discretize the problem domain, and a set of scattered nodes are used instead of meshing the domain of the problem. The meshless method is a new and interesting numerical technique. In recent years meshless techniques have attracted a lot of attention from researchers, and have gained importance for numerical solutions to the various types of engineering problems that are not suited to conventional numerical methods with a minimum of meshing or no meshing at all.[12]

Some meshless methods have been developed, such as smooth particle hydrodynamics methods,[13] the radial basis function,[14] the element free Galerkin (EFG) method,[15] the meshless local Petrov–Galerkin method,[16] the finite point method,[17−19] the meshless method based on the local boundary integral equation,[20] the reproducing kernel particle method,[21] the boundary element-free method,[22,23] the meshless method with complex variables,[24−27] and so on.

The EFG method is greatly developed and widely

*Project supported by the Natural Science Foundation of Ningbo City (Grant No. 2009A610014), the Natural Science Foundation of Zhejiang Province (Grant No. Y6090131), and the Research Foundation of Ningbo University of Technology (Grant No. 2008004).

†Corresponding author. E-mail: wangjufeng@gmail.com

© 2010 Chinese Physical Society and IOP Publishing Ltd

applied in various fields. To the best knowledge of the authors, this method has not been used for KdV equations. In this paper, the EFG method is firstly applied to the numerical solution of the KdV equation. In this method, the function over the solution domain does not require element connectivity, but only a set of nodes. The variational method is used to obtain the corresponding discrete equations, and the essential boundary conditions are enforced by the penalty method. The rest of the paper is organized as follows. In Section 2, we introduce the EFG method. In Section 3, the governing equation of the KdV equation is given, and the EFG method is implemented for including discrete equations of the problem. To present a clear overview of the method, in Section 4, we give two examples with analytical solutions, and solve them using the EFG method. The numerical results of these examples are in good agreement with the exact solutions. Section 5 ends this paper with a brief conclusion.

2. The EFG method

The EFG method, developed by Belytschko *et al.*,[15] employs the moving least-squares approximation to approximate the function $u(x)$ with $u^h(x)$. These approximants are constructed from three components: a weight function of compact support associated with each node, a basis, usually consisting of a polynomial, and a set of coefficients that depend on position.

2.1. Moving least-squares approximation

Now we consider the discretization of the domain given by a set of nodes. Each node has a corresponding nodal parameter u_I, which is a parameter governing the function $u(x)$ at that point. The approximation $u^h(x)$ is posed as a polynomial of order m with non-constant coefficients. In order to gain the expression of $u^h(x)$, Lancaster and Salkauskas[28] defined a local approximation by

$$u^h(x,\bar{x}) = \sum_{i=0}^{m} p_i(x)a_i(\bar{x}) \equiv P^{\mathrm{T}}(x)\alpha(\bar{x}), \tag{1}$$

where m is the number of terms in the basis, $p_i(x)$ are monomial basis functions, $a_i(x)$ are unknown coefficients, which are functions of the spatial coordinates x. The $P(x)$ is the vector form of $p_i(x)$, which denotes a basis consisting of a complete polynomial of order m and can be expressed in 1D as follows:

$$\begin{aligned} P^{\mathrm{T}}(x) &= \left[\begin{array}{cccc} p_1(x) & p_2(x) & \cdots & p_m(x) \end{array}\right] \\ &= \left[\begin{array}{cccc} 1 & x & \cdots & x^m \end{array}\right]. \end{aligned} \tag{2}$$

The $\alpha(x)$ is also the vector forms of $a_i(x)$ and has the form

$$\alpha^{\mathrm{T}}(x) = \left[\begin{array}{cccc} a_0(x) & a_1(x) & \cdots & a_m(x) \end{array}\right]. \tag{3}$$

To determine the unknown coefficient $\alpha(x)$, we minimize the weighted discrete L_2 norm given by

$$\begin{aligned} J &= \sum_{I=1}^{N} w(x-x_I)[u^h(x_I,x) - u_I]^2 \\ &= \sum_{I=1}^{N} w(x-x_I)[P^{\mathrm{T}}(x_I)\alpha(x) - u_I]^2, \end{aligned} \tag{4}$$

where $w(x-x_I)$ is a weight function, x_I and N are respectively the nodes and the number of nodes in the compacted supported domain of x, u_I refers to the nodal parameter of u at $x = x_I$.

By minimizing J in Eq. (4), the unknown parameter $\alpha(x)$ is equal to

$$\alpha(x) = A^{-1}(x)B(x)U, \tag{5}$$

where

$$A(x) = \sum_{I=1}^{N} w(x-x_I)P(x_I)P^{\mathrm{T}}(x_I), \tag{6}$$

$$B(x) = \left[\begin{array}{cccc} w(x-x_1)P(x_1), & w(x-x_2)P(x_2), & \cdots, & w(x-x_n)P(x_n) \end{array}\right], \tag{7}$$

$$U^{\mathrm{T}} = \left[\begin{array}{cccc} u_1 & u_2 & \cdots & u_n \end{array}\right]. \tag{8}$$

By substituting Eq. (5) into Eq. (1), the approximate function of $u(x)$ can be obtained

$$u^h(x) = u^h(x,x) = \sum_{i=0}^{m} p_i(x)a_i(x) = \sum_{I=1}^{N} \phi_I(x)u_I \equiv \Phi U, \tag{9}$$

where Φ is a matrix of shape function defined as

$$\Phi = [\phi_1(x),\ \phi_2(x),\ \ldots,\ \phi_N(x)] = P^{\mathrm{T}}(x)A^{-1}(x)B(x)U. \tag{10}$$

The derivatives of the unknown u are approximated by

$$\frac{\partial^k}{\partial x^k}u^h(x) = \sum_{I=1}^{N}\left[\frac{\partial^k}{\partial x^k}\phi_I(x)\right]u_I. \tag{11}$$

2.2. The weight functions

The weight function plays an important role in the EFG method, so the selection of an appropriate weight function is essential. The weight function $w(x-x_I)$ should be non-zero within only a small neighbourhood of x_I, called the domain of influence of node x_I, to generate a set of sparse discrete equations. The cubic spline weight function used in the present analysis can be written as a function of normalized radius r as follows:

$$w_I = w(x-x_I) \equiv w(r) = \begin{cases} \dfrac{2}{3} - 4r^2 + 4r^3, & r \le \dfrac{1}{2}; \\ \dfrac{4}{3} - 4r + 4r^2 - \dfrac{4}{3}r^3, & \dfrac{1}{2} < r \le 1; \\ 0, & r > 1 \end{cases} \tag{12}$$

with

$$r = \frac{d_I}{d_{m_i}}, \quad d_I = \|x - x_I\|, \quad d_{m_i} = d_{\max}c_I, \tag{13}$$

where $d_{\max}$ is a scaling parameter, the distance c_I is chosen such that the moment matrix $A(x)$ is not singular.

3. The governing equation and numerical scheme

The KdV equation in Cartesian coordinates has the following form[1]

$$u_t + \varepsilon u u_x + \mu u_{xxx} = 0, \tag{14}$$

where $u = u(x,t)$, ε, and μ are positive parameters, and the subscripts x and t denote the differentiations with respect to x and t.

Equation (14) has the initial conditions and boundary conditions as follows:

$$u(x,0) = f(x), \tag{15}$$

$$u(a,t) = \alpha_1(t), \quad u(b,t) = \alpha_2(t). \tag{16}$$

Now the EFG method will be implemented for obtaining the discrete equations of the problem. To obtain the discrete equations, it is first necessary to use a weak form of the differential equation. Because the EFG method does not interpolate the data, we use the penalty function method to deal with the boundary conditions. So by taking variation, we can have the following weak form of Eq. (14)

$$\int_\Gamma \delta u^{\mathrm{T}}(u_t + \varepsilon u u_x + \mu u_{xxx})\mathrm{d}\Gamma + \alpha\delta u^{\mathrm{T}}\cdot(u-\bar{u})|_{\Gamma_u} = 0, \tag{17}$$

where Γ denotes the domain of x, Γ_u denotes the boundaries, $\bar{u}$ are the values of u in the boundaries, α is a penalty parameter and usually equals $10^4 \sim 10^8$.

By the method of subsection integration, equation (17) can be written as

$$\int_\Gamma \delta u u_t \mathrm{d}\Gamma + \varepsilon\int_\Gamma \delta u\,(u u_x)\,\mathrm{d}\Gamma - \mu\int_\Gamma \delta u_x u_{xx}\mathrm{d}\Gamma + \alpha\delta u^{\mathrm{T}}\cdot(u-\bar{u})|_{\Gamma_u} = 0. \tag{18}$$

Using Eqs. (9) and (11), we have the approximations of u, u_x, u_{xx} and u_t as follows:

$$u^h = \sum_{I=1}^{N}\phi_I(x)u_I(t) = \Phi U(t), \tag{19}$$

$$u_x^h = \sum_{I=1}^{N}\left[\frac{\partial}{\partial x}\phi_I(x)\right]u_I(t) = \sum_{I=1}^{N}\phi_{I,x}(x)u_I(t) = \Phi_x\,U(t), \tag{20}$$

$$u_{xx}^h = \sum_{I=1}^{N}\left[\frac{\partial^2}{\partial x^2}\phi_I(x)\right]u_I(t) = \sum_{I=1}^{N}\phi_{I,xx}(x)u_I(t) = \Phi_{xx}\,U(t), \tag{21}$$

$$u_t^h = \sum_{I=1}^{N}\phi_I(x)\frac{\partial u_I(t)}{\partial t} = \Phi\dot{U}(t), \tag{22}$$

where $U(t) = [u_1(t),\ u_2(t),\ \cdots,\ u_N(t)]^{\mathrm{T}}$, $\dot{U}(t) = \partial U(t)/\partial t$, $\Phi = [\phi_1(x),\ \phi_2(x),\ \cdots,\ \phi_N(x)]^{\mathrm{T}}$, $\Phi_x = \partial\Phi/\partial x$, $\Phi_{xx} = \partial\Phi_x/\partial x$, $\phi_{I,x}(x) = \partial\phi_I(x)/\partial x$, $\phi_{I,xx}(x) = \partial\phi_{I,x}(x)/\partial x$, and Φ can be obtained through Eq. (10).

Substituting Eqs. (19)–(22) into the weak form (18) yields

$$\begin{aligned}\delta U(t)^{\mathrm{T}} K\dot{U}(t) &+ \delta U(t)^{\mathrm{T}} \int_\Gamma \varepsilon\,\Phi\cdot(uu_x)\,\mathrm{d}\Gamma \\ &- \delta U(t)^{\mathrm{T}} GU(t) + \delta U(t)^{\mathrm{T}} HU(t) \\ &- \delta U(t)^{\mathrm{T}} Q(t) = 0, \end{aligned} \tag{23}$$

where K, G and H are $N\times N$ matrices, whose values of the i-th row, j-th column are respectively

$$K_{ij} = \int_\Gamma \phi_i(x)\phi_j(x)\mathrm{d}\Gamma, \tag{24}$$

$$G_{ij} = \mu\int_\Gamma \phi_{i,x}(x)\phi_{j,xx}(x)\mathrm{d}\Gamma, \tag{25}$$

$$H_{ij} = \alpha\left[\phi_i(x)\phi_j(x)|_{x=a} + \phi_i(x)\phi_j(x)|_{x=b}\right]. \tag{26}$$

$Q(t)$ is an $N\times 1$ matrix, whose j-th row is

$$Q_j(t) = \alpha\left[\phi_j(x)\bar{u}|_{x=a} + \phi_j(x)\bar{u}|_{x=b}\right]. \tag{27}$$

According to the arbitrariness of $\delta U(t)$, equation (23) becomes

$$\begin{aligned}K\dot{U}(t) &+ \int_\Gamma \varepsilon\,\Phi\cdot(uu_x)\,\mathrm{d}\Gamma - GU(t) \\ &+ HU(t) - Q(t) = 0. \end{aligned} \tag{28}$$

We discretize the time derivative of Eq. (28) by using the usual finite difference formula and the space derivative by the Crank–Nicholson formula between two successive time levels n and $n+1$,

$$\begin{aligned}K\frac{U^{n+1}-U^n}{\Delta t} &+ \int_\Gamma \varepsilon\,\Phi\cdot\frac{(uu_x)^{n+1}+(uu_x)^n}{2}\mathrm{d}\Gamma \\ &+ (H-G)\frac{U^{n+1}+U^n}{2} - \frac{Q^{n+1}+Q^n}{2} = 0, \end{aligned} \tag{29}$$

where Δt is the time step, $U^n = U(n\Delta t)$, and so on.

The nonlinear term $(uu_x)^{n+1}$ in the above equation is literalized by using the following term[29]

$$(uu_x)^{n+1} = u^{n+1}(u_x)^n + u^n(u_x)^{n+1} - u^n(u_x)^n. \tag{30}$$

So equation (29) can be written as

$$K\frac{U^{n+1}-U^n}{\Delta t} + \int_\Gamma \varepsilon\,\Phi\cdot\frac{u^{n+1}(u_x)^n + u^n(u_x)^{n+1}}{2}\mathrm{d}\Gamma + (H-G)\frac{U^{n+1}+U^n}{2} - \frac{Q^{n+1}+Q^n}{2} = 0. \tag{31}$$

Substituting Eqs. (19) and (20) into Eq. (31) yields

$$K\frac{U^{n+1}-U^n}{\Delta t} + \int_\Gamma \varepsilon\,\Phi\cdot\frac{(U^n)^{\mathrm{T}}\left(\Phi_x\Phi^{\mathrm{T}} + \Phi\Phi_x^{\mathrm{T}}\right)U^{n+1}}{2}\mathrm{d}\Gamma + (H-G)\frac{U^{n+1}+U^n}{2} - \frac{Q^{n+1}+Q^n}{2} = 0. \tag{32}$$

Then we can obtain the discrete linear equations about U^{n+1}

$$\psi^n U^{n+1} = Z^n, \tag{33}$$

where

$$\begin{aligned}\psi^n &= K + \frac{\Delta t}{2}\int_\Gamma \varepsilon\,\Phi\cdot(U^n)^{\mathrm{T}}\left(\Phi_x\Phi^{\mathrm{T}} + \Phi\Phi_x^{\mathrm{T}}\right)\mathrm{d}\Gamma \\ &\quad + \frac{\Delta t}{2}(H-G), \end{aligned} \tag{34}$$

$$\begin{aligned}Z^n &= \left[K - \frac{\Delta t}{2}(H-G)\right]U^n \\ &\quad + \frac{\Delta t}{2}\left(Q^{n+1}+Q^n\right). \end{aligned} \tag{35}$$

Equation (33) is the discrete expression of the KdV equation. We can have the value of parameter U^{n+1} at any time through Eq. (33), and then by substituting U^{n+1} into Eq. (19), we can gain the approximation of the exact solution of the KdV equation.

4. Numerical examples

To test the efficiency of the EFG method for the KdV equation, we present two examples, which are chosen for their analytical solutions being known.

The discrete linear equations (33) are assembled by integrating over the domain of the problem using Gauss quadrature. To evaluate these integrals, it is necessary to define integration cells over the domain of the problem. In our examples, a regular arrangement of nodes is used with 100 nodes, and a cell structure is to set the quadrature cells equal to the intervals between the nodes. In each integration cell, a 4-Gauss-quadrature scheme is used to evaluate the stiffness matrix. Once the cells and corresponding quadrature points are defined, the discrete equations are assembled by looping over each quadrature point.

4.1. Example 1

We will solve the KdV equation in the following initial and boundary conditions

$$u(x,0) = 3c\left[\operatorname{sech}(Ax+D)\right]^2,$$
$$u(0,t) = u(2,t) = 0, \quad t > 0. \tag{36}$$

In this case, the KdV equation has the analytical solution as follows:

$$u(x,t) = 3c\left[\operatorname{sech}(Ax - Bt + D)\right]^2, \tag{37}$$

where $A = \frac{1}{2}\sqrt{\varepsilon c/\mu}, B = \varepsilon cA$.

We will use the EFG method to solve the above KdV equation. Computation is done with $\varepsilon = 1$, $\mu = 4.84 \times 10^{-4}$, $c = 0.3$, $D = -6$, $\Delta t = 0.0002$, $\alpha = 10^7$. The weight function is chosen to be the cubic spline weight function, and the bases are chosen with a complete polynomial of order 2. In Fig. 1, the numerical and exact solutions are plotted at $t = 0.5$. In Fig. 2, we plot the progress of the solitary for $t = 0.3$, $0.6, \ldots$, 1.8, which shows that a single soliton with amplitude $3c$, is moving from left to the right at a constant speed. From these figures, we can find that numerical results for the KdV equation are in good agreement with the exact solutions under the conditions (36).

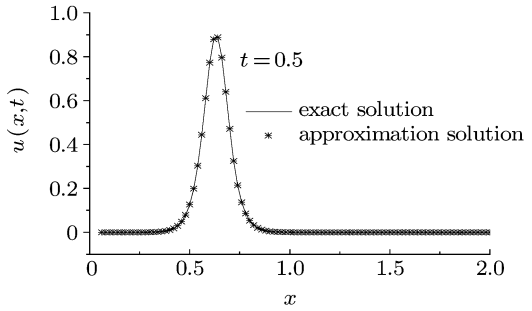


Fig. 1. Numerical and exact solutions for $t = 0.5$, $\varepsilon = 1$, $\mu = 4.84 \times 10^{-4}$, $c = 0.3$, $D = -6$, $\Delta t = 0.0002$, $\alpha = 10^7$.

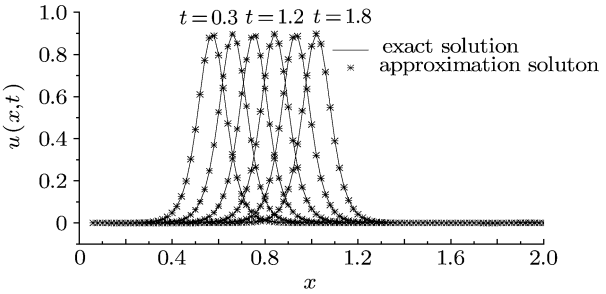


Fig. 2. Numerical and exact solutions for $t = 0.3, 0.6, \ldots, 1.8$, $\varepsilon = 1$, $\mu = 4.84 \times 10^{-4}$, $c = 0.3$, $D = -6$, $\Delta t = 0.0002$, $\alpha = 10^7$.

4.2. Example 2

In this example, we will deal with two soliton interaction solutions of the KdV equation under the initial and boundary conditions as follows:

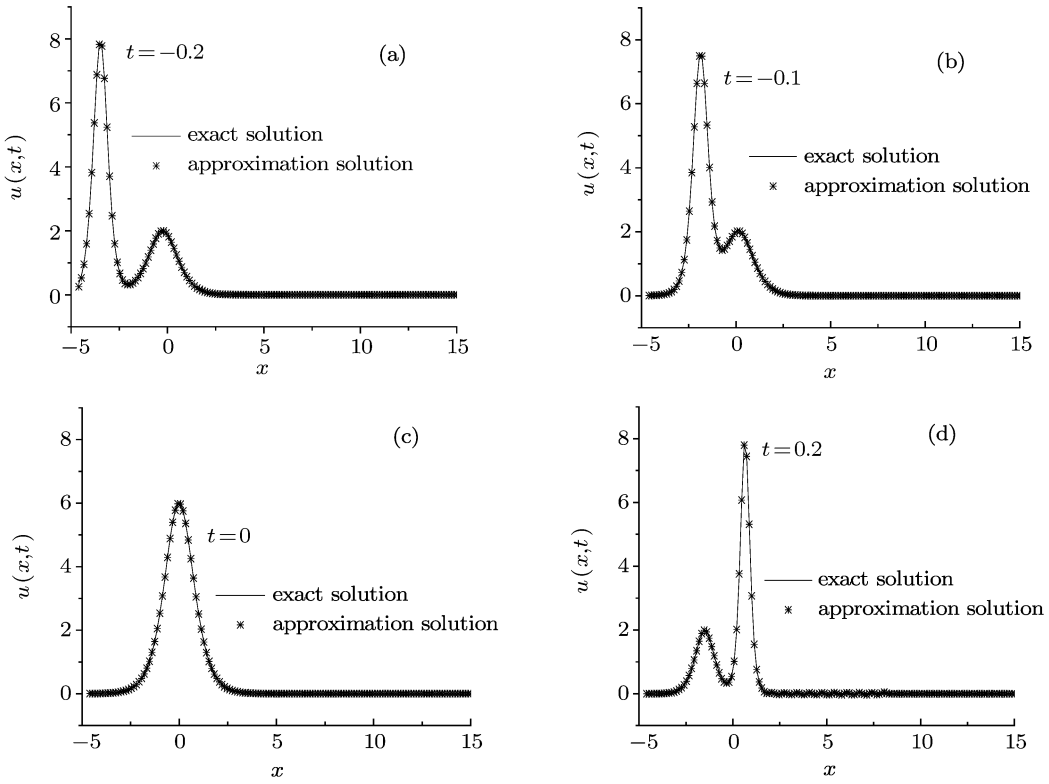


Fig. 3. Numerical and exact solutions for $t = -0.2, -0.1, 0, 0.2$, $\varepsilon = 6$, $\mu = 1$, $c = 0.3$, $D = -6$, $\Delta t = 0.0002$, $\alpha = 10^7$.

$$u(x,0) = \frac{12\left[3+4\cosh(2x)+\cosh(4x)\right]}{\left[3\cosh(x)+\cosh(3x)\right]^2}, \quad (38)$$

$$u(-5,t) = u(15,t) = 0. \quad (39)$$

Under these initial and boundary conditions, the KdV equation has the analytical solution as follows:

$$u(x,0) = \frac{12\left[3+4\cosh(2x-8t)+\cosh(4x-64t)\right]}{\left[3\cosh(x-28t)+\cosh(3x-36t)\right]^2}. \quad (40)$$

Numerical computation is done for $\varepsilon = 6$, $\mu = 1$, $\Delta t = 0.0002$, $\alpha = 10^7$. In Fig. 3, the numerical and exact solutions are plotted at different times, showing the progress of the two moving solitons. At the beginning, the solitons with higher amplitude stand on the left. Soon after the collision takes place, they gradually deform and finally merge into a single wave packet at $t = 0$. This wave packet, however, soon splits into two solitary waves. The soliton with higher amplitude moves faster than the soliton with smaller amplitude. Soon after, the soliton with higher amplitude stands on the right. From the numerical result, we also can find that numerical results are in good agreement with the exact solutions in this case.

5. Conclusion

The element-free Galerkin (EFG) method has been used for solving a kind of KdV equation. The meshless property of EFG is the most important advantage of this scheme over traditional mesh-dependent techniques, such as the finite difference method, finite element method and boundary element method. The meshless nature allows us to solve problems with non-regular geometry. The numerical results are in good agreement with the exact solutions, showing that the technique is accurate and efficient. The problems presented in this paper suggest that mesh-free approximation methods should be considered as one of the possible ways for solving these kinds of partial differential equations.

References

[1] Korteweg D J and Vries G de 1895 *Philos. Mag.* **39** 422

[2] Ames W (ed.) 1967 *Proceedings of Symposium Nonlinear Partial Differential Equations* (New York: Academic Press) pp. 223–258

[3] Gardner C S and Greene J M 1967 *Phys. Rev. Lett.* **19** 1095

[4] Gardner C S, Greene J M, Kruskal M D and Miura R M 1974 *Comm. Pure Appl. Math.* **27** 97

[5] Hirota R 1971 *Phys. Rev. Lett.* **27** 1192

[6] Hirota R 1973 *J. Math. Phys.* **14** 805

[7] Fornberg B and Whitham G B 1978 *Philos. Trans. Roy. Soc.* **289** 373

[8] Helal M A and Mehanna M A 2006 *Chaos, Solitons and Fractals* **28** 320

[9] Turabi Geyikli and Kaya Dogan 2005 *Appl. Math. Comput.* **169** 971

[10] Yan Z Y 2006 *Nonlinear Anal.* **64** 901

[11] Turabi Geyikli and Dogan Kaya 2005 *Appl. Math. Comput.* **169** 146

[12] Belytschko T, Krongauz Y and Organ D 1996 *Comput. Meth. Appl. Mech. Engng.* **139** 3

[13] Monaghan J J 1988 *Comput. Phys. Comm.* **48** 89

[14] Kansa E J 1990 *Comput. Math. Appl.* **19** 127

[15] Belytschko T, Lu Y Y and Gu L 1994 *Int. J. Numer. Meth. Engng.* **37** 229

[16] Atluri S N and Zhu T 1998 *Comput. Mech.* **22** 117

[17] Onate E, Idelsohn S and Zienkiewicz O C 1996 *Int. J. Numer. Meth. Engng.* **39** 3839

[18] Cheng R J and Cheng Y M 2008 *Appl. Numer. Math.* **58** 884

[19] Cheng R J and Cheng Y M 2007 *Acta Phys. Sin.* **56** 5569 (in Chinese)

[20] Dai B D and Cheng Y M 2007 *Acta Phys. Sin.* **56** 597 (in Chinese)

[21] Liu W K, Jun S and Zhang Y F 1995 *Int. J. Numer. Meth. Engng.* **20** 1081

[22] Cheng Y M and Chen M J 2003 *Acta Mech. Sin.* **35** 181 (in Chinese)

[23] Cheng Y M and Peng M J 2005 *Sci. Chin.* Ser. G **48** 641

[24] Cheng Y M and Li J H 2005 *Acta Phys. Sin.* **54** 44 (in Chinese)

[25] Chen Li and Cheng Y M 2008 *Acta Phys. Sin.* **57** 1 (in Chinese)

[26] Chen Li and Cheng Y M 2008 *Acta Phys. Sin.* **57** 50 (in Chinese)

[27] Peng M J and Cheng Y M 2009 *Eng. Anal. Bound. Elem.* **23** 77

[28] Lancaster P and Salkauskas K 1981 *Math. Comput.* **37** 141

[29] Rubin S G and Graves R A 1975 *Cubic Spline Approximation for Problems in Fluid Mehcanics* (Washington, DC: Nasa TR) R-436